RSC Advances

Manuscript ID: RA-ART-05-2015-008349.R3

Electronic Supplementary Information

Heteroleptic Iridium (III) complexes bearing coumarine moiety: an experimental and theoretical investigation†

Amit Maity, Rupa Sarkar and Kajal Krishna Rajak*

Inorganic Chemistry Section, Department of Chemistry, Jadavpur University, Kolkata, 700 032, India

* To whom correspondence should be addressed. Email: kajalrajak@hotmail.com

Jadavpur University

Table S1 Selected optimized geometrical parameters for **2** and **3** in the ground (S_0) and lowest lying triplet (T_1) excited states at B3LYP Levels using basis set aug-cc-pVDZ-pp for Ir atoms.

Bond Lengths (Å)				
	2		**3**	
	S_0	T_1	S_0	T_1
Ir1–O1	2.086	2.081	2.076	2.087
Ir1–N3	2.188	2.136	2.189	2.196
Ir1–N2	2.047	2.054	2.047	2.046
Ir1–N1	2.185	2.201	2.184	2.182
Ir1–C12	2.023	2.015	2.022	2.021
Ir1–C1	2.038	2.058	2.035	2.055
Bond Angles (°)				
	2		**3**	
	S_0	T_1	S_0	T_1
O1–Ir1–N3	88.0	84.3	87.9	87.9
N3–Ir1–N1	95.9	95.8	95.5	95.5
N1–Ir1–C1	79.1	78.8	79.2	79.2
N2–Ir1–C12	80.2	80.4	80.3	80.2
O1–Ir1–N1	84.4	90.1	84.8	84.4
N1–Ir1–N2	175.6	171.3	176.0	176.0
C1–Ir1–C12	88.3	87.7	88.2	88.3
C1–Ir1–O1	87.6	85.3	87.6	87.3
C12–Ir1–N1	99.2	95.5	99.2	99.1
C1–Ir1–N2	96.5	93.2	96.8	96.8
C12–Ir1–O1	173.8	170.0	173.5	173.4
N2–Ir1–O1	95.6	92.7	95.2	95.3
C1–Ir1–N3	173.7	168.3	173.4	173.3
N2–Ir1–N3	88.4	92.5	88.4	88.3
C12–Ir1–N3	96.3	103.1	96.5	96.6

Table S2 Frontier Molecular Orbital Composition (%) in the Ground State for [Ir(2-pypy)$_2$(L^2)], **2**

Orbital	Energy (eV)	Contribution (%)				Main bond type
		Ir	2-pypy	HL^2		
				Imine	Aromatic system	
LUMO+5	–1.190	0	16	2	83	π^* (2-pypy) + π^*(HL^2)
LUMO+4	–1.340	1	3	0	97	π^* (2-pypy) + π^*(HL^2)
LUMO+3	–1.720	5	0	0	96	π^*(HL^2)
LUMO+2	–1.770	3	1	0	96	π^*(HL^2)
LUMO+1	–1.900	1	75	22	2	π^* (2-pypy) + π^*(HL^2)
LUMO	–2.100	2	73	25	0	π^*(2-pypy) + π^*(HL^2)
HOMO	–5.490	40	30	4	27	d(Ir) + π(2-pypy) + π(HL^2)
HOMO–1	–5.650	43	31	0	26	d(Ir) + π(2-pypy) + π(HL^2)
HOMO–2	–5.810	38	13	1	48	d(Ir) + π(2-pypy) + π(HL^2)
HOMO–3	–6.140	6	82	5	7	π(2-pypy)
HOMO–4	–6.480	13	10	0	77	d(Ir) + π(HL^2)
HOMO–5	–6.570	16	25	0	59	d(Ir) + π(2-pypy) + π(HL^2)

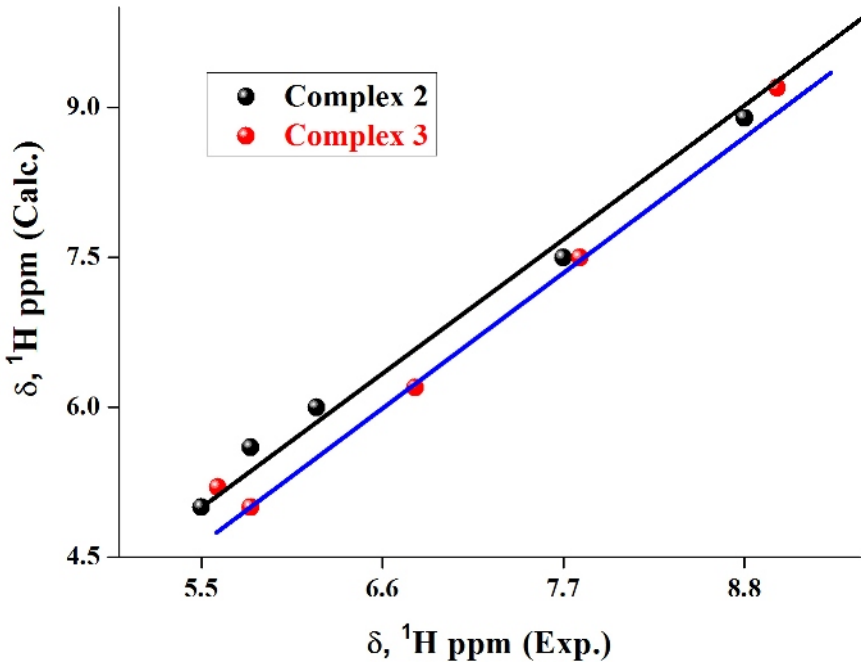

Fig. S1 (a) Linear correlation between the experimental and calculated ^{1}H NMR chemical shifts of **complex 2** and **complex 3**.

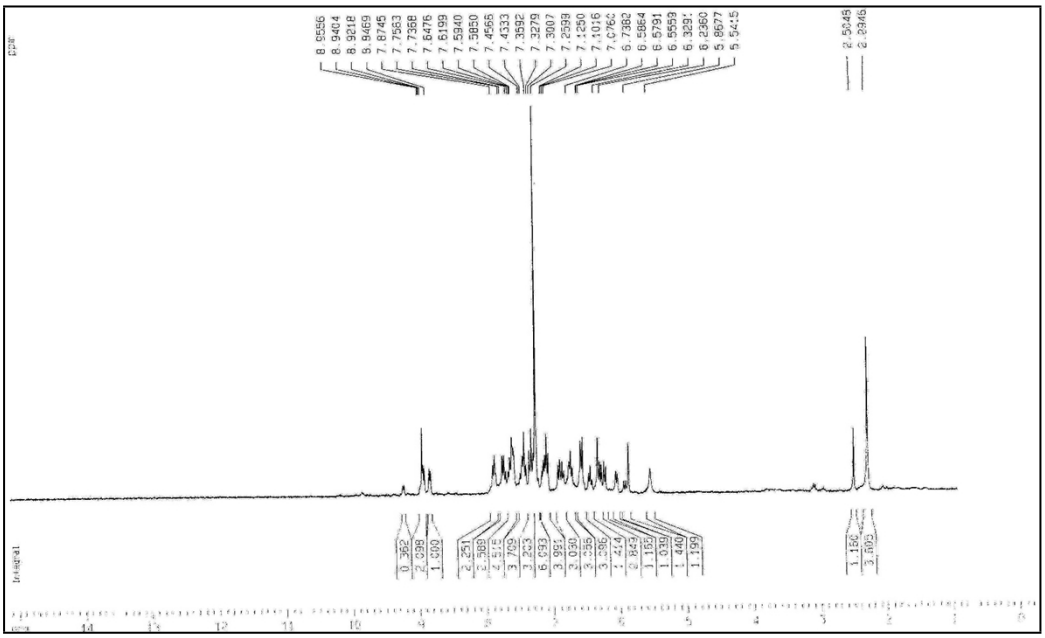

Fig. S1 (b) ^{1}H NMR spectrum of complex **2** in $CDCl_3$ solution.

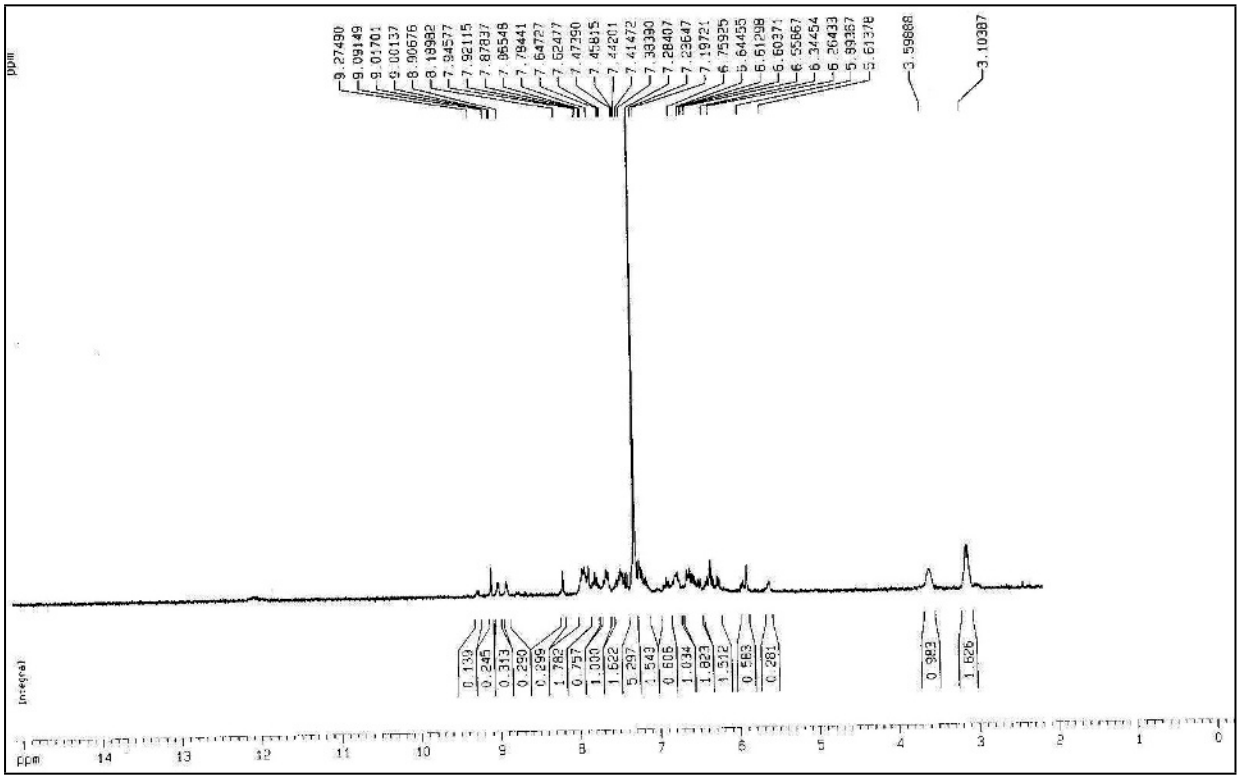

Fig. S1 (c) ^{1}H NMR spectrum of complex **3** in $CDCl_3$ solution.

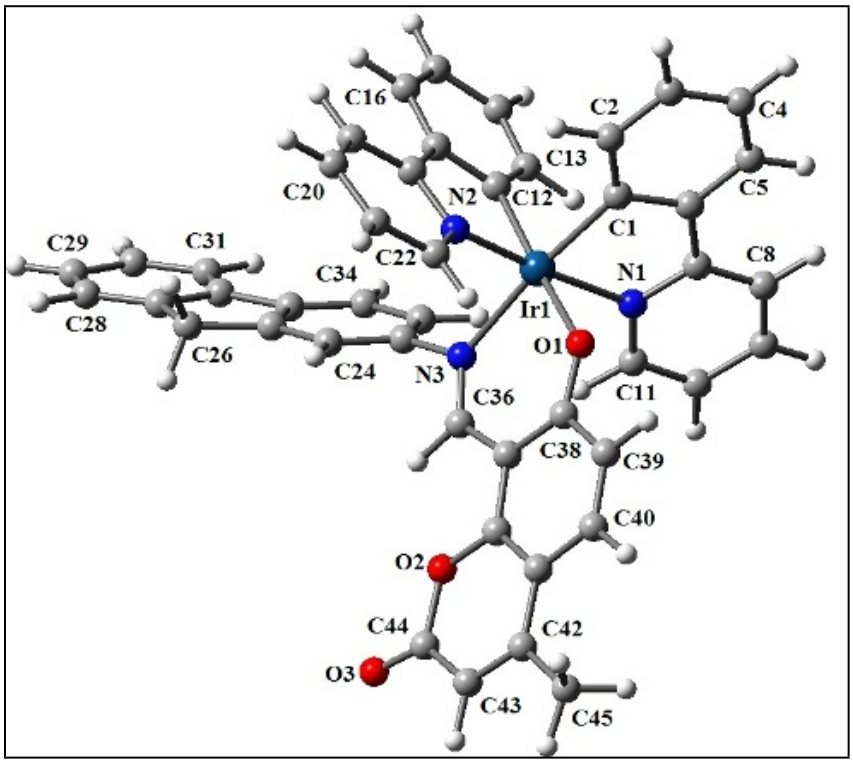

Fig. S2 Optimized molecular structure of [Ir(2-pypy)$_2$(L^2)], **2** at S_0 state. (Ir: Cyan, N: Blue, O: Red, C: Grey, H: White).

Table S3 Frontier Molecular Orbital Composition (%) in the Ground State for [Ir(2-pypy)$_2$(L^3)], **3**

Orbital	Energy (eV)	Contribution (%)				Main bond type
		Ir	2-pypy	HL^3		
				Imine	Aromatic system	
LUMO+5	–1.340	0	0	2	98	π* (2-pypy)+ π* (HL^3)
LUMO+4	–1.720	4	2	0	95	π* (2-pypy)+ π*(HL^3)
LUMO+3	–1.770	3	2	1	93	π*(HL^3)
LUMO+2	–1.870	1	65	28	6	π* (2-pypy)+ π*(HL^3)
LUMO+1	–2.020	0	95	4	1	π* (2-pypy)
LUMO	–2.170	1	78	19	1	π*(2-pypy)+ π*(HL^3)
HOMO	–5.480	35	38	3	24	d(Ir)+π(2-pypy)+π(HL^3)
HOMO–1	–5.640	19	62	0	19	d(Ir)+π(2-pypy)+π(HL^3)
HOMO–2	–5.690	35	49	1	16	d(Ir)+π(2-pypy)+π(HL^3)
HOMO–3	–5.850	37	15	1	47	d(Ir)+π(2-pypy)+π(HL^3)
HOMO–4	–6.490	12	9	0	79	d(Ir)+ π(HL^3)
HOMO–5	–6.570	19	26	0	55	d(Ir)+π(2-pypy)+π(HL^3)

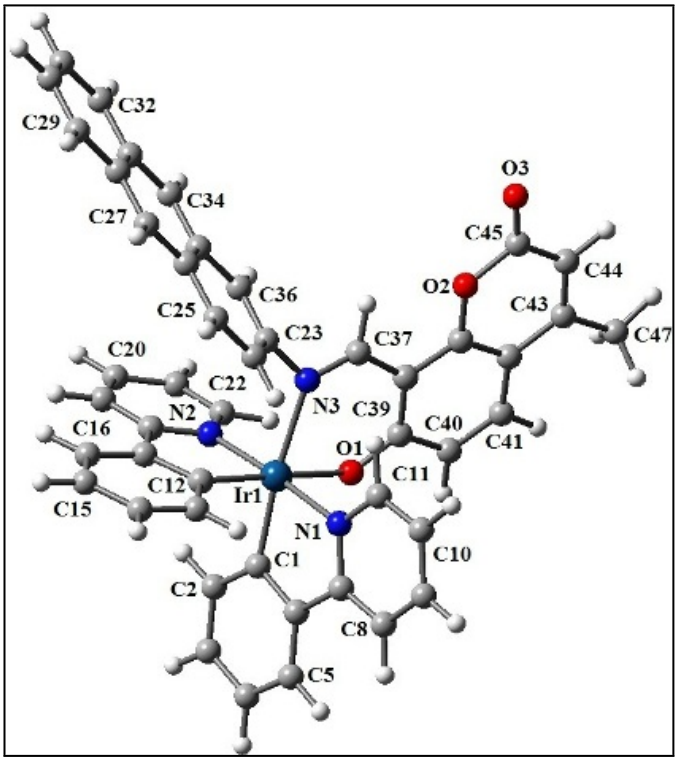

Fig. S3 Optimized molecular structure of [Ir(2-pypy)$_2$(L^3)], **3** at S_0 state. (Ir: Cyan, N: Blue, O: Red, C: Grey, H: White).

Table S4 Main calculated optical transition for the complex [Ir(2-pypy)$_2$(L^2)]**, 2** with composition in terms of molecular orbital contribution of the transition, vertical excitation energies, and oscillator strength in dichloromethane

Transition	Composition	E (eV)	Oscillator strength (f)	CI	λ_{theo} (nm)	Assign	λ_{exp} (nm)
$S_0 \rightarrow S_1$	HOMO → LUMO (93%)	2.7692	0.0351	0.682	448	^{1}MLCT / ^{1}ILCT/ ^{1}LLCT	451
	HOMO → LUMO+1 (3%)			–0.109		^{1}ILCT/ ^{1}LLCT	
$S_0 \rightarrow S_{12}$	HOMO–3 → LUMO (6%)	3.5451	0.0212	0.171	350	^{1}ILCT/ ^{1}LLCT	363
	HOMO–1 → LUMO+5 (3%)			0.102		^{1}ILCT/ ^{1}LLCT	
	HOMO→ LUMO+5 (87%)			0.660		^{1}MLCT/ ^{1}ILCT/ ^{1}LLCT	
$S_0 \rightarrow S_{50}$	HOMO–11 → LUMO (3%)	4.5248	0.1258	0.101	274	^{1}MLCT / ^{1}ILCT/ ^{1}LLCT	263
	HOMO–6 → LUMO+3 (7%)			0.189		^{1}ILCT/ ^{1}LLCT	
	HOMO–5→ LUMO+5 (3%)			–0.106		^{1}ILCT/ ^{1}LLCT	
	HOMO–4 → LUMO+5(52%)			0.513		^{1}MLCT / ^{1}ILCT/ ^{1}LLCT	
	HOMO→ LUMO+8 (7%)			–0.185		^{1}ILCT/ ^{1}LLCT	
	HOMO → LUMO+11 (3%)			0.120		^{1}MLCT / ^{1}ILCT/ ^{1}LLCT	
	HOMO → LUMO+12 (8%)			–0.199		^{1}MLCT / ^{1}ILCT/ ^{1}LLCT	

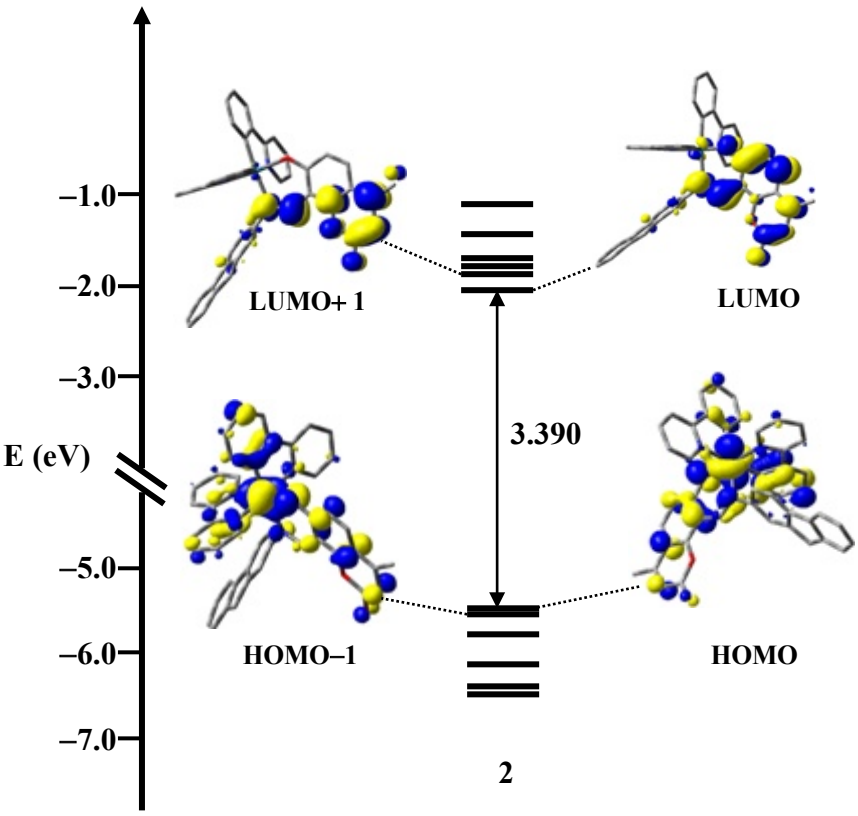

Fig. S4 Partial molecular orbital diagram with some isodensity frontier molecular orbital mainly involved in the electronic transitions for complex [Ir(2-pypy)$_2$(L^2)], **2**.

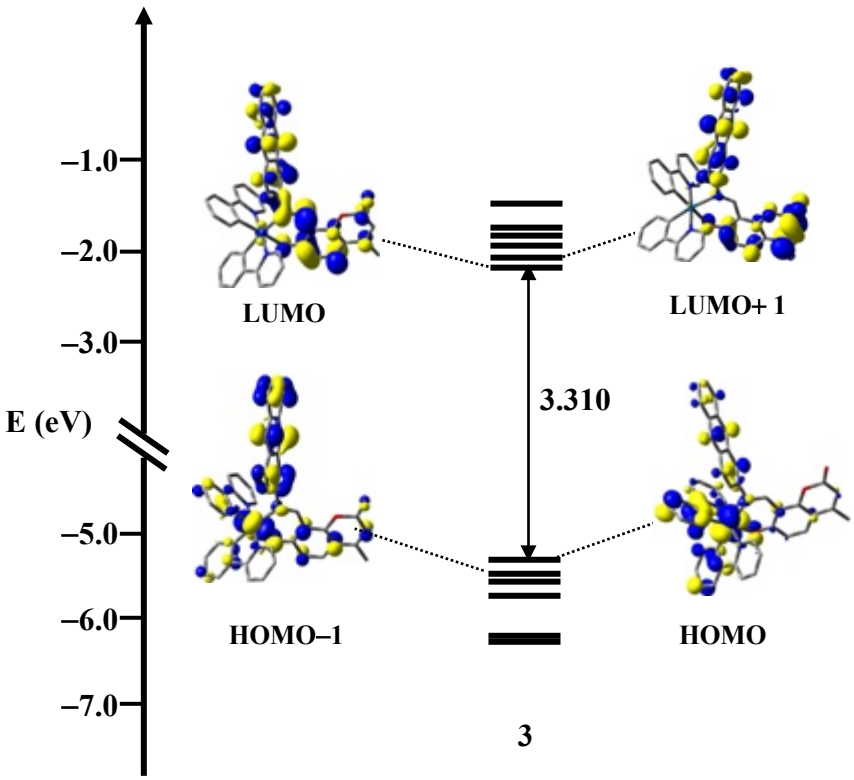

Fig. S5 Partial molecular orbital diagram with some isodensity frontier molecular orbital mainly involved in the electronic transitions for complex [Ir(2-pypy)$_2$(L^3)], **3**.

Table S5 Main calculated optical transition for the complex [Ir(2-pypy)$_2$(L^3)], **3** with composition in terms of molecular orbital contribution of the transition, vertical excitation energies, and oscillator strength in dichloromethane

Transition	Composition	E (eV)	Oscillator strength (f)	CI	λ_{theo} (nm)	Assign	λ_{exp} (nm)
$S_0 \rightarrow S_1$	HOMO-1 → LUMO (5%)	2.7210	0.0667	0.156	456	^{1}ILCT/ ^{1}LLCT	454
	HOMO → LUMO (69%)			0.586		^{1}MLCT/ ^{1}ILCT/ ^{1}LLCT	
	HOMO → LUMO+1 (15%)			–0.270		^{1}ILCT/ ^{1}LLCT	
	HOMO → LUMO+2 (5%)			–0.158		^{1}ILCT/ ^{1}LLCT	
	HOMO → LUMO+3 (3%)			–0.107		^{1}ILCT/ ^{1}LLCT	
$S_0 \rightarrow S_{18}$	HOMO–3 → LUMO+2 (7%)	3.4249	0.0107	–0.191	362	^{1}ILCT/ ^{1}LLCT	360
	HOMO–3 → LUMO+3(34%)			0.410		^{1}MLCT/ ^{1}ILCT/ ^{1}LLCT	
	HOMO–3 → LUMO+4 (14%)			-0.267		^{1}MLCT/ ^{1}ILCT/ ^{1}LLCT	
	HOMO–2 → LUMO+1 (2%)			–0.105		^{1}MLCT/ ^{1}ILCT/ ^{1}LLCT	
	HOMO–2 → LUMO+2 (3%)			0.112		^{1}MLCT/ ^{1}ILCT/ ^{1}LLCT	
	HOMO–2 → LUMO+5 (3%)			–0.116		^{1}MLCT/ ^{1}ILCT/ ^{1}LLCT	
	HOMO-1 → LUMO+2(4%)			0.148		^{1}MLCT/ ^{1}ILCT/ ^{1}LLCT	
	HOMO-1 → LUMO+3 (5%)			–0.161		^{1}MLCT/ ^{1}ILCT/ ^{1}LLCT	
	HOMO-1 → LUMO+4(4%)			–0.126		^{1}MLCT/ ^{1}ILCT/ ^{1}LLCT	
	HOMO-1 → LUMO+5(3%)			0.117		^{1}MLCT/ ^{1}ILCT/ ^{1}LLCT	
	HOMO→ LUMO+5(14%)			0.261		^{1}MLCT/ ^{1}ILCT/ ^{1}LLCT	
$S_0 \rightarrow S_{50}$	HOMO–9 → LUMO (61%)	4.3927	0.0123	0.552	282	^{1}MLCT / ^{1}ILCT/ ^{1}LLCT	259
	HOMO–9→ LUMO+1 (10%)			–0.228		^{1}ILCT/ ^{1}LLCT	
	HOMO–7 → LUMO+2(4%)			0.141		^{1}ILCT/ ^{1}LLCT	
	HOMO–6 → LUMO+2(3%)			–0.129		^{1}ILCT/ ^{1}LLCT	
	HOMO–2 → LUMO+7 (2%)			0.103		^{1}MLCT / ^{1}ILCT/ ^{1}LLCT	

Table S6 Calculated triplet excited state of [Ir(2-pypy)$_2$(L^3)], **3** in dichloromethane based on the lowest lying triplet state geometry. Main calculated vertical transitions with compositions in terms of molecular orbital contribution of the transition, vertical excitation energies and oscillator strength

Complex	Excita-tion	Composition	E (eV)	Oscillator Strength (f)	CI	Assign	λ_{exp} (nm)
3	1	HOMO – 8 → LUMO	2.6110 eV (475 nm)	0.0402	0.10471	^{3}ILCT	471
		HOMO – 6 → LUMO			–0.10181	^{3}ILCT	
		HOMO – 2 → LUMO			0.28062	^{3}ILCT	
		HOMO → LUMO + 1			0.20081	^{3}ILCT	
		HOMO → LUMO+2			0.11247	^{3}ILCT	
		HOMO → LUMO+3			–0.10885	^{3}ILCT	
		HOMO–1 → LUMO			0.21629	^{3}ILCT	
		HOMO–1 → LUMO+1			–0.27048	^{3}ILCT	
		HOMO–1→ LUMO+2			0.34306	^{3}ILCT	
		HOMO–1→ LUMO+3			–0.11413	^{3}ILCT	
		HOMO → LUMO+6			0.17999	^{3}ILCT	
		HOMO–7→ LUMO			–0.14542	^{3}ILCT	
		HOMO–2 → LUMO+1			0.10396	^{3}ILCT	
		HOMO-1 → LUMO+1			0.29340	^{3}ILCT	
		HOMO-1 → LUMO+2			–0.17370	^{3}ILCT	
		HOMO-1 → LUMO+3			–0.14011	^{3}ILCT	
		HOMO-1 → LUMO+4			0.12243	^{3}ILCT	
		HOMO→ LUMO+1			0.16375	^{3}ILCT	
		HOMO → LUMO+2			0.26723	^{3}ILCT	
		HOMO → LUMO+3			–0.19445	^{3}ILCT	
		HOMO → LUMO+4			0.21550	^{3}ILCT	
		HOMO → LUMO+5			–0.13981	^{3}ILCT	
	2	HOMO–7→ LUMO	2.7634eV (448 nm)	0.0259	–0.62724	^{3}ILCT	440
		HOMO–2 → LUMO+1			0.18858	^{3}ILCT	
		HOMO→ LUMO+1			0.68975	^{3}ILCT	
		HOMO → LUMO+2			0.13814	^{3}ILCT	
		HOMO → LUMO+5			–0.10024	^{3}ILCT	

^{1}MLCT / ^{1}ILCT	Hole	Electron

454 nm	**3**	S_1 w = 0.69 2.721 eV (0.06) t_{2g}– π→ π*	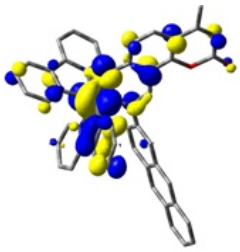	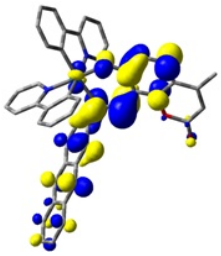
360 nm		S_{18} w = 0.34 3.424 eV (0.01) t_{2g}– π → π*	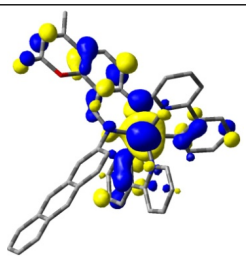	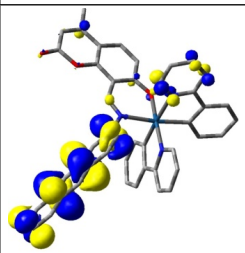
259 nm		S_{50} w = 0.61 4.392 eV (0.01) t_{2g}– π → π*	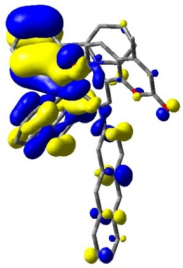	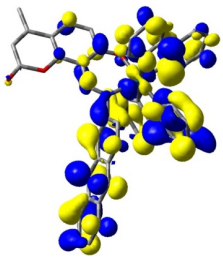

Fig. S6 Natural transition orbitals (NTOs) for the complex [Ir(2-pypy)$_2$(L^3)], **3** illustrating the nature of optically active singlet excited states in the absorption bands 454, 360 and 259 nm. For each state, the respective number of the state, transition energy (eV), and the oscillator strength (in parentheses) are listed. Shown are only occupied (holes) and unoccupied (electrons) NTO pairs that contribute more than 25% to each excited state. All transitions are mixed ^{1}MLCT/^{1}ILCT character: charge is transferred from mainly t_{2g} – π hole orbital to the π*orbital of the ligands.

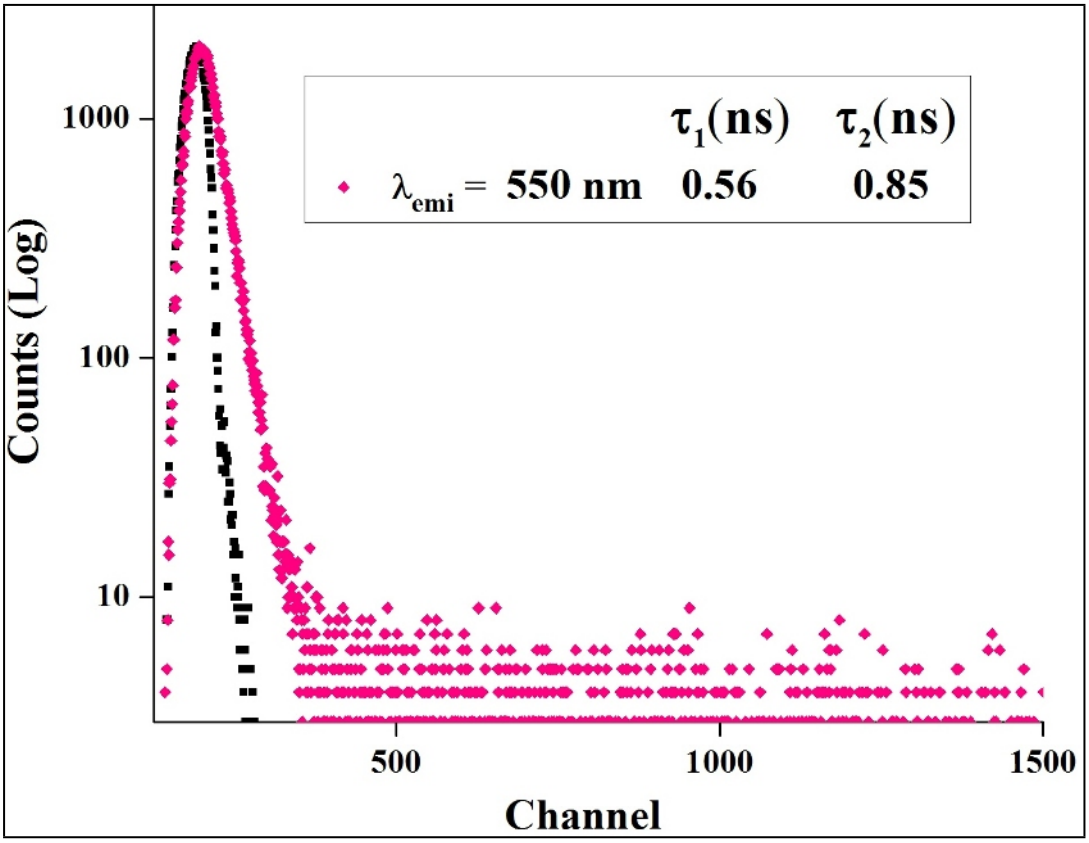

Fig. S7 Changes in the time-resolved photoluminescence decay of complexes [Ir(2-pypy)$_2$(L^1)], **1** in dichloromethane at room temperature obtained with 450 nm excitation. The emission at 543 nm was monitored.

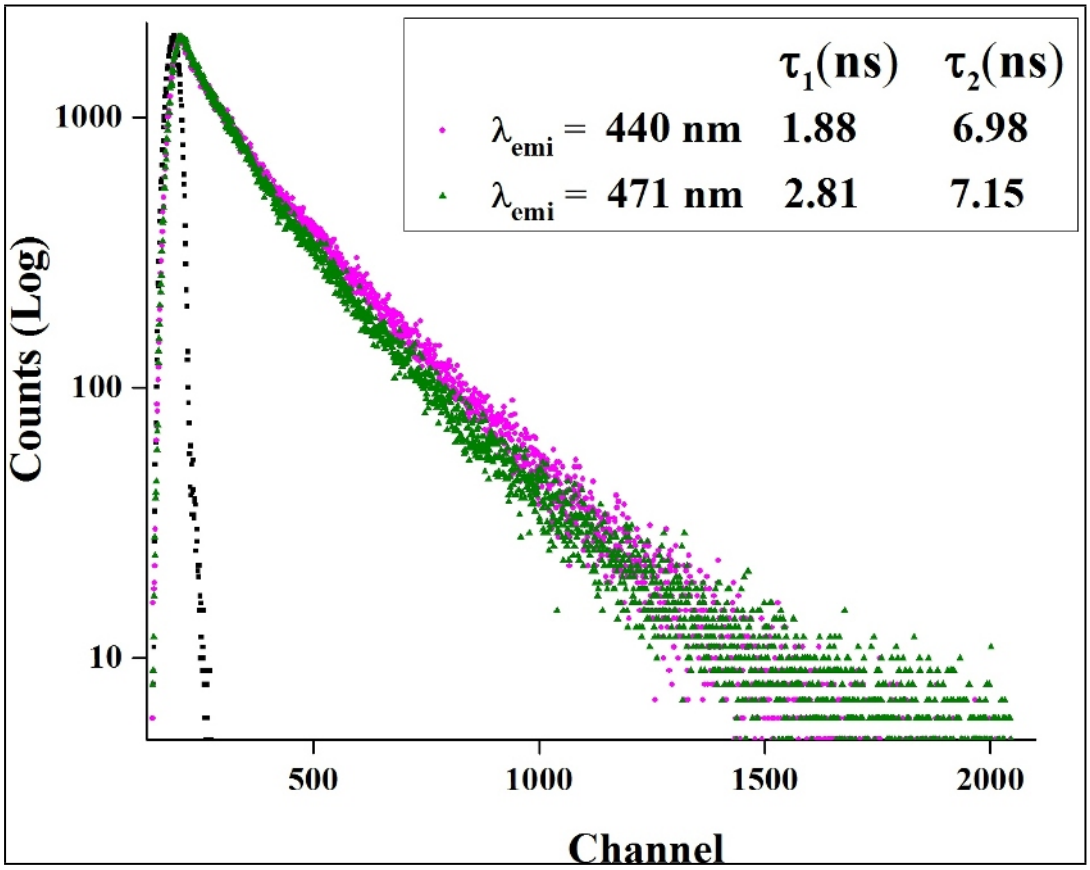

Fig. S8 Changes in the time-resolved photoluminescence decay of complexes [Ir(2-pypy)$_2$(L^3)], **3** in dichloromethane at room temperature obtained with 450 nm excitation. The emission at 440 and 471 nm was monitored.

Fig. S9 TG curve of complex $[Ir(2\text{-pypy})_2(L^1)].2H_2O$, **1.**$2H_2O$